AIP | Review of Scientific Instruments

# Closed, heated reaction chamber design for dynamic high-temperature x-ray-diffraction analyses of gas/solid displacement reactions

Michael S. Haluska, Robert L. Snyder, Kenneth H. Sandhage, and Scott T. Misture

Citation: Rev. Sci. Instrum. **76**, 126101 (2005); doi: 10.1063/1.2136076
View online: http://dx.doi.org/10.1063/1.2136076
View Table of Contents: http://rsi.aip.org/resource/1/RSINAK/v76/i12
Published by the American Institute of Physics.

# Closed, heated reaction chamber design for dynamic high-temperature x-ray-diffraction analyses of gas/solid displacement reactions

Michael S. Haluska,[a] Robert L. Snyder, and Kenneth H. Sandhage
*School of Materials Science and Engineering, Georgia Institute of Technology, Atlanta, Georgia 30350*

Scott T. Misture
*New York State College of Ceramics at Alfred University, Alfred, New York 14802*

(Received 6 June 2005; accepted 1 August 2005; published online 14 December 2005)

A closed, x-ray transparent chamber for containing a hot reactive gas (generated from an internal condensed source) has been designed and evaluated for use in dynamic x-ray-diffraction analysis of a gas/solid displacement reaction. The chamber consisted of a square-bottom base and lid machined from dense pyrolytic graphite. The base contained a flat pedestal, upon which $SiO_2$ microshells (the reactant oxide) were placed, raised above adjacent cavities holding Mg flakes (the condensed precursor to the reactive gas). Upon heating to 650 °C, the Mg evaporated and reacted with the $SiO_2$ inside the sealed chamber. By passing incident and diffracted x rays through the vertical side walls of the chamber and by blocking undesired graphite-diffracted x rays with platinum, the $Mg(g)/SiO_2(s)$ displacement reaction could be tracked with time. This is the first use of dynamic high-temperature x-ray diffraction analysis to monitor the progress of a displacement reaction involving a reactant gas that was generated and confined within a closed reaction chamber. © *2005 American Institute of Physics.* [DOI: 10.1063/1.2136076]

High-temperature x-ray diffraction (HTXRD) is an attractive analytical method for the dynamic evaluation of phase evolution and of reaction kinetics for solid/solid and fluid/solid reactions.[1–5] HTXRD has frequently been used to analyze gas/solid reactions involving reactant gas species that also exist as gases at room temperature (e.g., $O_2$, $N_2$, $H_2$, and CO).[6–8] However, a number of reactions of scientific and technological interest involve reactant species that can only be generated as gases with appreciable vapor pressures at elevated temperatures (i.e., such species are stable as solids or liquids at room temperature). HTXRD analyses of these types of gas/solid reactions are complicated by the need to generate and confine the hot reactive gas in the vicinity of the solid reactant for a sufficient time as to enable evaluation of the progress of reaction. New experimental designs are needed to allow for HTXRD analyses of such reactions.

Gas/solid displacement reactions have recently been used by Sandhage and co-workers to change the chemistry, but not the shapes, of microscopic silica-based structures generated by aquatic microorganisms known as diatoms.[9–13] Diatoms are single-celled algae that assemble intricate three-dimensional (3D) microshells (frustules) comprised of silica nanoparticles.[14,15] Tens of thousands of diatom species exist on the planet, with each species forming a 3D frustule with a particular shape that is decorated with a species-specific (genetically precise) pattern of fine (down to nanoscale) features.[14,15] Sustained reproduction of a given diatom can yield enormous numbers of descendant diatoms (e.g., 40 reproduction cycles can yield $2^{40}$ or more than $1\times10^{12}$ diatoms) with frustules of similar complex 3D morphology.[16] The massive parallelism, genetic precision, and environmental compatibility of such biological self-assembly are highly attractive characteristics for the low-cost manufacturing of nanostructured devices. However, the silica-based chemistry of diatom frustules is not appropriate for a wide variety of device applications. Gas/silica displacement reactions have recently been used to convert $SiO_2$-based frustules into MgO or $TiO_2$.[9–13] In the case of MgO, the magnesium vapor generated upon heating magnesium to 900 °C was used to alter silica frustules according to the following net displacement reaction:

$$2Mg(g) + SiO_2 \Rightarrow 2MgO(s) + \{Si\}. \quad (1)$$

{Si} refers to silicon in elemental form or dissolved within a Mg-bearing phase.[9,10,13] While this reaction has yielded MgO-based frustule replicas, the dynamic evaluation (such as by HTXRD analysis) of phase evolution during the course of such reaction at $\leqslant$900 °C has not been reported.

The purpose of this article is to describe the design and use of a closed, heated, x-ray transparent chamber capable of containing a reactive gas (generated from a condensed source within the chamber) for the dynamic HTXRD analysis of a gas/solid displacement reaction [i.e., the oxidation-reduction reaction between $Mg(g)$ and $SiO_2(s)$]. To the authors' knowledge, this is the first time that HTXRD analysis has been used to track the progress of such a displacement reaction within a closed reaction chamber.

The selection of materials for the reaction chamber was restricted by several criteria. The chamber material needed to be (i) transparent to x rays, (ii) inert with respect to hot magnesium gas, (iii) machinable or formable, (iv) resistant to thermal degradation at elevated temperature, (v) thermally conductive, and (vi) nonporous [in order to contain the reac-

[a]Electronic mail: mike.haluska@mse.gatech.edu

 

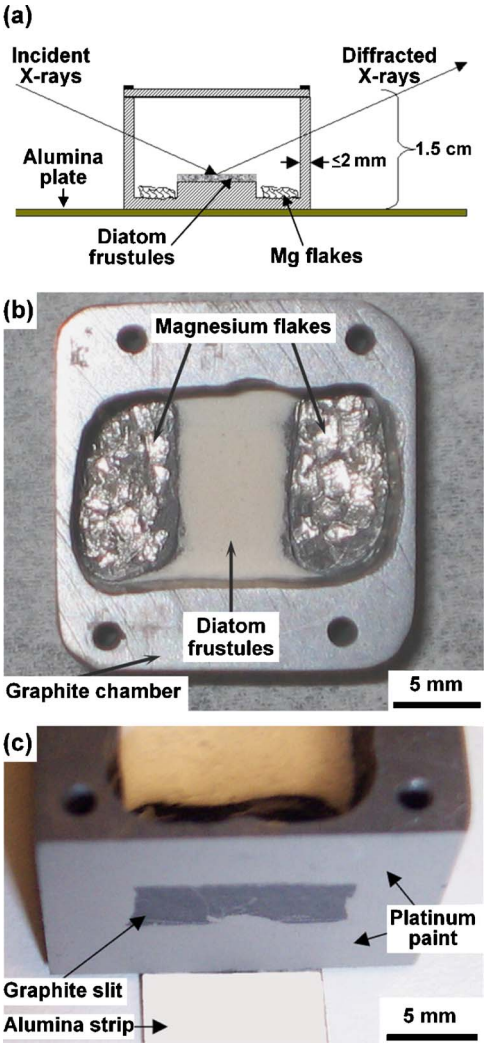


FIG. 1. (a) Schematic illustration (side view) of the graphite reaction chamber. (b) Optical image (top-down view) of the base of the graphite reaction chamber containing the diatom frustules and magnesium flakes. (c) Optical image of the graphite "slit" created between platinum painted on the exiting vertical sidewall of the graphite base.

tant Mg($g$) and to allow for good thermal conduction]. Among the low-absorption solid elements (Li, Be, B, and C) or compounds (the carbides, nitrides, or oxides of Li, Be, or B), graphite was a particularly attractive choice. Polycrystalline graphite is quite machinable, does not react with Mg($g$) to form compounds at ambient pressures,[17] is thermally stable at elevated temperatures, is thermally conductive,[18] and is commercially available in high purity and dense forms. Mo $K\alpha$ x rays can also penetrate 4 mm of dense graphite while retaining more than 60% of the incident intensity.[19]

A graphite reaction chamber was machined from isostatistically pressed, binder-free pyrolytic graphite (ATJ grade, 99.5% dense, Becker-Brothers Carbon, Maywood, Illinois). A schematic drawing of a side view of the reaction chamber is shown in Fig. 1(a). The chamber consisted of a square base (outer dimensions of 2 cm wide $\times$2 cm long $\times$1.5 cm tall) and lid (2 cm wide $\times$2 cm long $\times$2 mm thick). The top surface of the base and the bottom surface of the graphite lid were polished flat using 2000 grit SiC-impregnated paper (Buehler, Ltd., Lake Bluff, IL). Four holes were drilled and threaded into the base and the lid so as to allow for attachment with stainless-steel screws and washers (18-8 stainless, McMaster Carr, Atlanta, GA). The base contained a flat pedestal (7 mm wide $\times$10 mm long) raised 7 mm above two adjacent cavities. $SiO_2$-based diatom frustules, obtained as diatomaceous earth from a local vendor, were mixed into slurry with isopropanol and then deposited onto the pedestal to a thickness of 2 mm using a spatual. Magnesium flakes (>99.8% purity, 0.5 mm thick $\times$2 mm wide, Alfa Aesar, Ward Hill, MA) were loaded into the adjacent cavities using tweezers. The molar $Mg:SiO_2$ ratio placed in the chamber was 1.5:1. An optical image of the base of the reaction chamber containing the diatom frustules and magnesium flakes is shown in Fig. 1(b). After placing the silica and magnesium reactants in the base of the graphite chamber, the lid was secured to the base and the chamber was placed within a high-temperature x-ray-diffraction (HTXRD) system.

A customized HTXRD system[20] was used for these experiments. This system consisted of a Siemens D500 diffractometer with a vertical theta-theta goniometer, a controlled-atmosphere furnace, an MBRAUN position-sensitive detector with a silver cathode (10° $2\theta$ window, P-10 gas), and 0.1° divergence slits to yield an x-ray spot size of approximately $5\times5$ mm$^2$. The furnace was comprised of two platinum/20% rhodium hemispherical coils that were designed to fit together so as to surround the sample upon closing the furnace. The heated zone of the furnace was 4.1 cm in diameter. The graphite reaction chamber was placed on a thin alumina plate ($100\times20\times1$ mm$^3$ thick) and fixed in position with a small amount of platinum paste (Engelhard Corp., Iselin, NJ). This assembly was then placed in the center of the furnace. The temperature at the center of the furnace was calibrated with the use of NIST standards (SRM760, $K_2SO_4$, $K_2CrO_4$, NIST, Gaithersburg, MD). Upon closing the graphite reaction chamber into the o-ring-sealed furnace, the furnace was purged with a flowing 4% $H_2$/He atmosphere. The graphite reaction chamber was then heated in the flowing 4% $H_2$/He atmosphere (to avoid oxidation of the graphite) at a rate of 30 °C/min to 650 °C, whereupon sequential isothermal diffraction measurements were conducted. X rays were passed into and out of the sealed furnace through a beryllium window located along an arc at the top of the furnace. Diffraction patterns were collected using Mo $K\alpha$ radiation (0.7093 Å, 17.7 KeV) with 50 seconds of lag time between each measured pattern. As indicated by the schematic image in Fig. 1(a), the incident and diffracted x rays were passed through the vertical sidewalls of the graphite reaction chamber. By machining the sidewalls to a thickness of $\leqslant$2 mm, more than 60% of the incident and diffracted Mo $K\alpha$ x rays could pass through the graphite in both sidewalls.[19] Although the sidewalls could be machined to as thin as 0.35 mm for enhanced x-ray beam penetration, such thin-walled cells were fragile and would often break during handling of the cell at room temperature or burst under the pressure of Mg vapor generated within the sealed cell upon heating. The selected 1–2 mm wall thickness was a compromise between the performance (x-ray penetration) and dura-

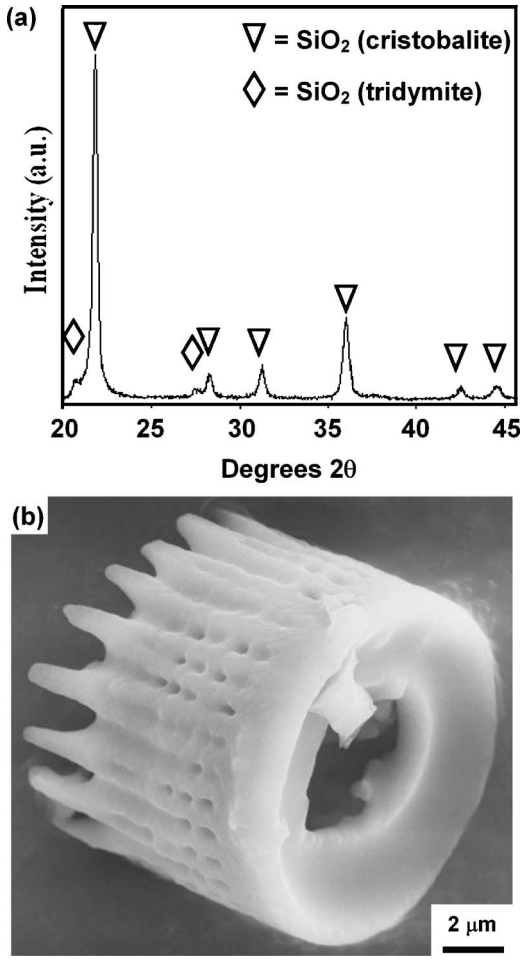


FIG. 2. (a) Room-temperature (Cu $K\alpha$) XRD pattern obtained from the starting diatom frustules (as diatomaceous earth). (b) Representative secondary electron image of a starting diatom frustule.

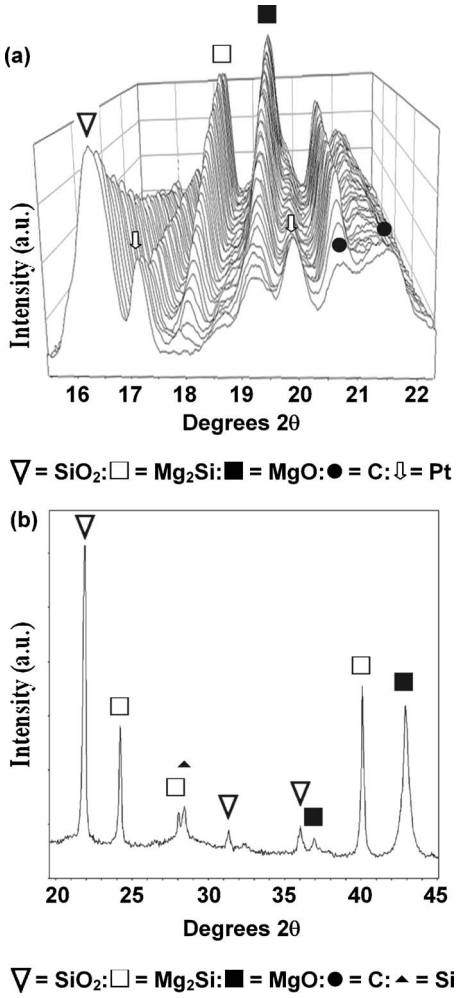


FIG. 3. (a) Isothermal high-temperature diffraction patterns obtained during the reaction of $SiO_2$ diatom frustules with Mg gas at 650 °C (40 patterns for a total of 205 min of reaction time at the final pattern). (b) Room-temperature (Cu $K\alpha$) XRD pattern obtained from the same specimens in (a) after cooling to room temperature and removal from the graphite chamber.

bility of the cell. In order to reduce undesired graphite diffraction from the front vertical sidewall of the chamber, platinum paste (Engelhard, Iselin, NJ) was painted on the outside surface of the exit vertical sidewall so as to leave a "slit" of graphite where the beam could pass [see Fig. 1(c)].

A room-temperature x-ray-diffraction pattern and a representative secondary electron image of the starting silica-based diatom frustules are shown in Figs. 2(a) and 2(b), respectively. The XRD pattern reveals predominant peaks for the $\alpha$-cristobalite polymorph of silica.[21] The image in Fig. 2(b) reveals that the $SiO_2$-based frustules possessed a hollow, cylindrical shape. Because these frustules were physically separated from the magnesium flakes within the graphite chamber, the frustules could only react with the gaseous form of magnesium generated upon heating to 650 °C. The equilibrium pressure of magnesium vapor over liquid magnesium at 650 °C is 3.1 torr, which is much higher than the magnesium vapor pressure required for the net reaction (1) to proceed.[17,22] However, the formation of magnesium carbides was not thermodynamically favored under these conditions; that is, the graphite cell was inert with respect to $Mg(g)$.[17,22]

The HTXRD pattern obtained at 650 °C is shown in Fig. 3(a). A standard XRD pattern (using Cu $K\alpha$ radiation) obtained from the reacted frustules of Fig. 3(a), after cooldown to room temperature and removal from the graphite chamber, is shown in Fig. 3(b). Diffraction peaks for $SiO_2$ (as $\beta$-cristobalite), MgO, and $Mg_2Si$ were clearly detected in Fig. 3(a), along with the peaks for graphite and platinum (Note that the $\alpha$-cristobalite polymorph of $SiO_2$ is converted into the $\beta$-cristobalite polymorph via a rapid displacive phase transformation during heat up to 650 °C.[23] The silicon detected in Fig. 3(b) was also present in Fig. 3(a), although the Si (220) diffraction peak overlapped with a graphite diffraction peak in Fig. 3(a). The two diffraction peaks for graphite shown in Fig. 3(a) resulted from the diffraction of Mo $K\alpha$ x rays with the horizontal surface of the graphite pedestal located under the $SiO_2$ frustules and with the front vertical sidewall of the graphite chamber.[21] The relative intensities of these undesired graphite diffraction peaks were reduced by optimizing the chamber and slit geometries. The diffraction from the graphite sidewall may be isolated by considering the geometry of the cell. Part of the beam incident on the vertical (left) sidewall of the graphite cell in Fig. 1(a) diffracted from the point of contact with this vertical sidewall. The remainder (nondiffracted part) of the beam continued on through the vertical graphite sidewall and in-

teracted with the sample. The beam diffracting from the incident (left) graphite wall in Fig. 1(a) traveled a different path and exited at the right side of the cell at a higher vertical position than the beam that had not been diffracted by the left sidewall. An increase in the lateral dimension [the left-to-right length in Fig. 1(a)] of the cell resulted in an increased likelihood that the beam diffracted by the left graphite sidewall would be attenuated by the painted platinum shielding surrounding the slit on the right sidewall in Fig. 1(a). By increasing the lateral cell dimension and by reducing the slit size, the intensities of sidewall-diffracted graphite peaks were significantly reduced. Peaks due to diffraction from the platinum on the right sidewall in Fig. 1 were also detected in Fig. 3(a).

The relative intensity of the $SiO_2$ diffraction peak decreased, and the relative intensities of the MgO and $Mg_2Si$ peaks increased, with increasing reaction time in Fig. 3(a). These changes in relative intensity were consistent with the following reactions:

$$2\mathrm{Mg}(g) + \mathrm{SiO_2}(s) \Rightarrow 2\mathrm{MgO}(s) + \mathrm{Si}(s), \quad (2)$$

$$2\mathrm{Mg}(g) + \mathrm{Si}(s) \Rightarrow \mathrm{Mg_2Si}(s). \quad (3)$$

Although a small amount of MgO had formed during heat up to 650 °C via reaction (2), the onset of $Mg_2Si$ formation via reaction (3) occurred shortly after reaching this temperature. The gradual, monotonic changes in the relative intensities of the $SiO_2$, MgO, and $Mg_2Si$ diffraction peaks in Fig. 3(a) indicated that the reaction of silica frustules with magnesium gas inside the closed, heated graphite chamber could be carefully tracked with time at 650 °C by HTXRD analyses. This is the first time that dynamic HTXRD analysis has been used to monitor the extent of a displacement reaction between solid and gas reactants that were confined within a closed, heated chamber. This approach opens the door to dynamic HTXRD analyses of a variety of reactions involving gaseous reactants that possess appreciable vapor pressures only at elevated temperatures (i.e., gaseous reactants that are generated by heating condensed sources).

The financial support provided for this work by the Air Force Office of Scientific Research (Dr. Joan Fuller and Dr. Hugh De Long, program managers) is gratefully acknowledged.

[1] B. J. Chen, M. A. Rodriguez, S. T. Misture, and R. L. Snyder, Physica C **217**, 367 (1993).
[2] A. P. Wilkinson, J. S. Speck, A. K. Cheetham, S. Natarajan, and J. M. Thomas, Chem. Mater. **6**, 750 (1994).
[3] A. K. Sheridan and J. Anwar, Chem. Mater. **8**, 1042 (1996).
[4] P. Norby, A. N. Christensen, and J. C. Hanson, Inorg. Chem. **38**, 1216 (1999).
[5] C. Lind, A. P. Wilkinson, C. J. Rawn, and E. A. Payzant, J. Mater. Chem. **12**, 990 (2002).
[6] M. Ozawa and C.-K. Loong, Catal. Today **50**, 329 (1999).
[7] N. Wakiya, S.-Y. Chun, K. Shinozaki, and N. Mizutani, J. Solid State Chem. **149**, 349 (2000).
[8] M. D. Dolan and S. T. Misture, Rigaku J. **21**, 12 (2004).
[9] K. H. Sandhage, *et al.*, Adv. Mater. (Weinheim, Ger.) **14**, 429 (2002).
[10] K. H. Sandhage, M. B. Dickerson, P. M. Huseman, F. M. Zalar, M. R. Rondon, and E. C. Sandhage, Ceram. Eng. Sci. Proc. **23**, 653 (2002).
[11] R. R. Unocic, F. M. Zalar, P. M. Sarosi, Y. Cai, and K. H. Sandhage, Chem. Commun. (Cambridge) **7**, 796 (2004).
[12] K. H. Sandhage *et al.*, Int. J. Appl. Ceram. Technol. **2**, 317 (2005).
[13] Y. Cai, S. M. Allan, F. M. Zalar, and K. H. Sandhage, J. Am. Ceram. Soc. **88**, 2005 (2005).
[14] F. E. Round, R. M. Crawford, and D. G. Mann, *The Diatoms: Biology & Morphology of the Genera* (Cambridge University Press, Cambridge, 1990).
[15] M. Hildebrand and R. Wetherbee, *Progress in Molecular and Subcellular Biology* (Springer, Berlin, 2003), pp. 11–57.
[16] V. Martin-Jezequel, M. Hildebrand, and M. A. Brezezinski, J. Phycol. **36**, 821 (2000).
[17] I. Barin, *Thermochemical Data of Pure Substances*, 1st ed. (VCH, Weinheim, 1989), pp. 994, 1000, 100, 1014, 1505.
[18] Y. S. Touloukian, R. W. Powell, C. Y. Ho, and P. G. Klemens, *Thermal Conductivity, Nonmetallic Solids*, Thermophysical Properties of Matter (Plenum, New York, 1970), Vol. 2 pp. 31–41.
[19] B. D. Cullity, *Elements of X-ray Diffraction*, 2nd ed. (Addison-Wesley, Reading, MA, 1978), p. 512.
[20] S. T. Misture, Meas. Sci. Technol. **14**, 1091 (2003).
[21] JCPDS-International Center on Diffraction Data, Powder Diffraction File Card Nos. 39-1425 for $\alpha$-cristobalite, 27-605 for $\beta$-cristobalite, 45-946 for MgO, 35-0773 for $Mg_2Si$, 27-1402 for Si (2005).
[22] K. V. Gourishankar, M. Karaminezhad Ranjbar, and G. R. St. Pierre, J. Phase Equilib. **14**, 601 (1993).
[23] W. D. Kingery, H. K. Bowen, and D. R. Uhlmann, *Introduction to Ceramics*, 2nd ed. (Wiley, New York, 1976), p. 87.